The neural basis of visual attentional inhibition

K-112093

Specific Aim 1

Neural basis of distractor resistance during visual working memory maintenance

Background

Visual working memory has to cope with the interference posed by the temporally co-occurring distractor stimuli. It is widely believed that distractor resistance might be accomplished by the same feedback selection processes that are active during visual perception and leading to enhanced and suppressed global visual cortical processing of task relevant and irrelevant information, respectively. In fact, previous research provided strong evidence for top-down modulation of target and distractor processing in the visual cortex during WM encoding and the observed effects were consistent with the biased competition model of visual attentional selection. Human neuroimaging studies revealed that early ERP responses (including the P1 and N1 component) as well as feature/object selective visual cortical fMRI responses are increased and decreased for the to-be-memorized and irrelevant visual information, respectively. Furthermore, it was also shown that the efficacy of attentional selection during encoding, as reflected in the strength of modulation of visual cortical processing, predicted working memory performance.

However, whether analogous attentional-selection-mediated distractor exclusion processes can account for interference resistance during WM maintenance remained an open question. Behavioural research provided strong evidence for delay distractor interference effects when fine detail object information—allowing no abstract level coding—had to be stored in WM and the delay distractor objects matched the maintained object's category, i.e. congruent distractors. For example, irrelevant face stimuli—but not scenes or gratings—presented during the WM maintenance period significantly impair identity discrimination performance in case of unfamiliar faces. Within the framework of the sensory recruitment model of WM, similar attentional selection processes are proposed to account for interference resistance during encoding and maintenance. According to this model, sensory processes that are responsible for the perception and encoding of the to-be-remembered visual stimuli will be kept active during the WM delay period via a sustained WM-content-dependent attentional selection template. Therefore, interference resistance during WM maintenance depends on how efficiently WM-content-dependent feedback selection processes can detract attention from and/or suppress processing of distractor stimuli and thus mitigate the interference between the WM target and distractor representations. Previous electrophysiological recordings from behaving animals and human neuroimaging studies provided support for the WM-content-dependent sustained modulation of neural activity during WM maintenance in the visual cortex as well as in the fronto-parietal regions that are thought to represent the source of this feedback modulation. However, research aimed at investigating WM-content-dependent modulation of the neural responses to task irrelevant stimuli appearing during the WM delay revealed conflicting results. Human EEG studies found decreased early ERP responses (P1 and N1 components) to congruent as compared to incongruent distractors and the results were interpreted as evidence for WM-content-based attentional suppression of task-irrelevant visual information during WM maintenance. Whereas, in several previous fMRI studies congruent delay distractor objects evoked

stronger responses in the object-selective visual cortical areas than incongruent distractors, which results appears to be consistent with previous behavioural findings showing WM-content-guided allocation of visual attention in visual search tasks performed during the WM maintenance period.

Importantly, a recent line of experimental results obtained using electrophysiological recordings from the prefrontal and parietal cortical areas of behaving monkeys opened a new perspective on the neural basis of delay distractor resistance. Using a numerosity short-term memory task, involving objects presented in the central visual field, it was revealed that congruent distractor stimuli evoke strong neural responses in the prefrontal cortex, interrupting sustained WM-content-specific representations. Furthermore, it was also found that WM content and distractor representations were actively separated via frequency specific coding within the fronto-parietal cortical network and frontal mnemonic representations were reactivated after distractor had disappeared. These results are consistent with the dynamic models of WM representation maintenance as well as a large body of human neuroimaging results indicating that WM representations can be stored in a hidden, activity salient format and thus WM-content-specific sustained activities within the sensory cortex are not a requirement for successful WM maintenance. These studies also showed that in case when distractors were anticipated during the delay period, sustained-activity-based maintenance of the WM representations in the visual cortex was ceased before appearance of distractors and was reactivated after their disappearance.

Hypothesis: Taken together, these findings raise the intriguing possibility that in the central visual field, where spatial selection is inefficient, delay distractor resistance might be achieved via active separation of distractor representations from the WM content representations, rather than filtering of the irrelevant information based on sustained global attentional selection. Importantly, such representation separation account of distractor interference elimination could explain previous findings showing increased fMRI responses in object selective visual cortical areas, but would be at odds with previous EEG findings showing suppression of early ERP responses to delay distractors.

We addressed this question using a series of EEG and fMRI experiments investigating the neural processing of congruent and incongruent distractors presented during the delay period of a WM task requiring maintenance of unfamiliar face identity or grating orientation information. Representation separation account of distractor resistance would predict enhanced fMRI responses in visual cortical areas selectively involved in coding the WM content representation as well as increased P3b component of the ERP responses, reflecting memory access and reactivation related processes in case of congruent as compared to incongruent distractors. On the other hand, if interference is eliminated via sustained global attentional filtering of distractor information, both visual cortical fMRI responses and early ERP components, including the P1 and N1 are expected to be decreased for congruent distractors.

Methods

Stimuli and Procedure

During EEG and fMRI experiments participants performed a retrocued Sternberg working memory task with faces and simple grating patterns, with distracting face and grating stimuli appearing in the delay period (Fig. 1.1). On each trial, two compound face-grating stimuli as sample stimuli (SAMPLE1 and SAMPLE2) were presented after which a SYMBOLIC RETRO-CUE appeared, which indicated whether the two faces (Face WM trials) or the two gratings (Grating WM trials) were to be probed at

the end of the trial. Evidently, participants did not know in advance which category would be relevant when they saw the sample stimuli, and they were explicitly instructed to try to memorize both gratings and faces. After a jittered delay, a DELAY DISTRACTOR with red fixation disc could appear. After an additional delay, the PROBE, which was also a compound face-grating stimulus, was displayed. The irrelevant image component in the probe was always different from all previous stimuli in the current trial. The relevant image component (as indicated by the retro-cue) was either also different from all others of the trial ('new' trials), or it was one of the probe stimuli from the current trial reoccurring ('old' trials). Participants had to indicate whether they saw an old or a new probe.

With respect to the delay distractor, there were 3 trial types in EEG Experiment 1. During no-distractor trials, the only event was the fixation disc turning red, no stimulus was presented. On face-distractor and grating-distractor trials, a face or a grating was drawn from the stimulus pool that was different from all other stimuli in the current trial. In EEG Experiment 2. and fMRI Experiment there were 2 trial types including no-distractor and face-distractor trials for EEG Experiment 2. and face-distractor and grating-distractor trials for fMRI Experiment. Distractors were always different from all the stimuli used in the trial.

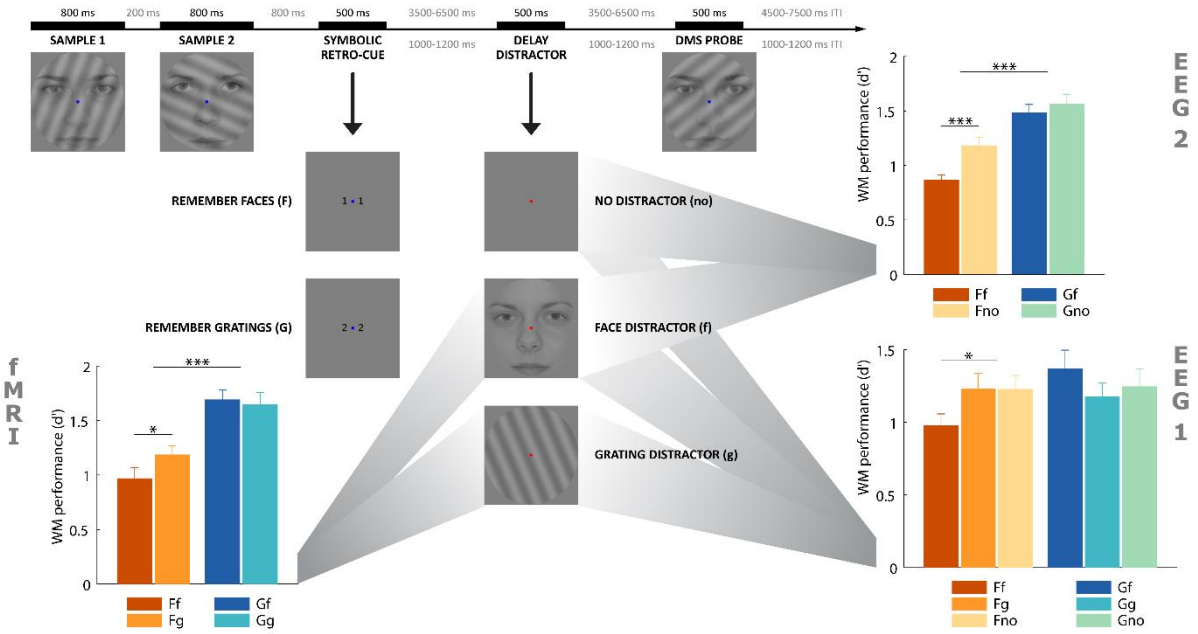

Figure 1.1. Experimental design and grand average WM performance (d') (±SE) of a retrocued Sternberg working memory task using compound face-grating stimuli with distracting face and grating stimuli appearing in the delay period for EEG and fMRI experiments. Durations below the time axis are indicated for EEG experiments only if they differed from those used in fMRI Experiment. Ff: FWMT with face (congruent) distractor; Fg: FWMT with grating (incongruent) distractor; Gf: GWMT with face (incongruent) distractor; Gg: GWMT with grating (congruent) distractor; Fno: FWMT without distractor; Gno: GWMT without distractor; *p < 0.05, ***p < 0.001.

EEG Experiments

Data acquisition and analysis. Data of 20 and 54 healthy young adult participants were analysed for EEG Experiment 1. and EEG Experiment 2., respectively. During both experiments, EEG data was recorded using a BrainAmp Standard amplifier, controlled by BrainVision Recorder 1.2 (Brain

Products GmbH, Munich, Germany). For the first experiment, a 64-channel ActiCap active electrode system was used with two amplifier heads, in the Experiment 2 a 96-channel ActiCap system was applied (Brain Products), fitted on an elastic cap (EasyCap GmbH, Munich, Germany). The EEG signal was sampled at 1000 Hz in Experiment 1. and 2500 Hz in Experiment 2. To test how distractor congruency affects processing of the delay distractors, difference of distractor-related EEG between Ff and Gf conditions was evaluated using paired-samples t-tests with spatio-temporal cluster-based permutation testing for both Experiment 1. and Experiment 2. Additionally, the difference of distractor-related alpha-band (8-13 Hz) EEG activity was also tested using the same statistical approach in the case of Experiment 2. Clusters with P values lower than 0.05 (P_{Clus}<0.05) were considered significant.

fMRI Experiment

Data acquisition. Data were acquired on a Siemens Magnetom Prisma 3T MRI scanner (Siemens Healthcare, Erlangen, Germany) at the Brain Imaging Centre, Research Centre for Natural Sciences, Hungarian Academy of Sciences. All head elements of the standard Siemens 64-channel head-neck receiver coil were applied. The protocol consisted of T1-weighted 3D MPRAGE anatomical imaging using 2-fold in-plane GRAPPA acceleration (TR/TE/FA = 2300 ms/3 ms/9°; FOV = 256 mm; isotropic 1 mm spatial resolution). A blipped-controlled aliasing in parallel imaging simultaneous multi-slice gradient-echo-EPI sequence was used for functional measurements with 6-fold slice acceleration, using full brain coverage with an isotropic 2 mm spatial resolution and a TR of 710 ms, without in-plane parallel imaging. A partial Fourier factor of 7/8 was used to achieve a TE of 30 ms. Image reconstruction was performed using the Slice-GRAPPA algorithm with LeakBlock kernel.

Data analysis. Data of 33 healthy young adult participants were analysed. Preprocessing and analysis of the imaging data were performed using the SPM12 toolbox (Wellcome Trust Centre for Neuroimaging, London, UK) as well as custom-made scripts running on MATLAB R2015a (The MathWorks Inc., Natick, MA, USA). Standard preprocessing steps including motion correction, normalization to MNI space, and spatial smoothing with a Gaussian filter of 5 mm FWHM followed by 128-second high-pass filtering were performed to prepare fMRI data for first- and second-level statistics.
For first-level statistical analysis we used a standard voxelwise General Linear Model (GLM) with HRF-convolved stimulus regressors for face (f) and grating (g) distractor conditions in cases of face (F) and grating (G) working memory tasks. The first-level contrast images of the estimated beta weights of the defined regressors (Ff, Fg, Gf, Gg) served as input for the second-level whole-brain and region-of-interest (ROI) based random effects *t* statistics.

Results

Behavioural results

When face identity information had to be stored in working memory (face working memory task–FWMT) in all three experiments we found significantly reduced WM performance in trials with congruent distractors (faces, Ff) as compared to those with incongruent distractors (gratings, Fg) (Fig. 1.1). On the other hand, no distractor congruency effect was found in the grating working memory task (GWMT). Furthermore, there was no significant difference in WM performance between incongruent (Fg, Gf) and no distractor trials (Fno, Gno) in the EEG Experiment 1. Reaction times were not affected by distractor congruency.

EEG results

Experiment 1. The first EEG experiment was aimed at uncovering how distractor congruency affects processing of the delay distractors. In both FWMT and GWMT, distractor congruency effects on EEG responses to delay distractor stimuli were confined to the later stages of visual information processing, starting around 200 ms (Fig. 1.2). The most pronounced effect was found in the time window corresponding to the P3b component. Early P1 and N1 ERP components evoked by the face or grating distractors did not differ between the congruent and incongruent trials. These results are consistent with the pattern separation account of delay distractor interference elimination.

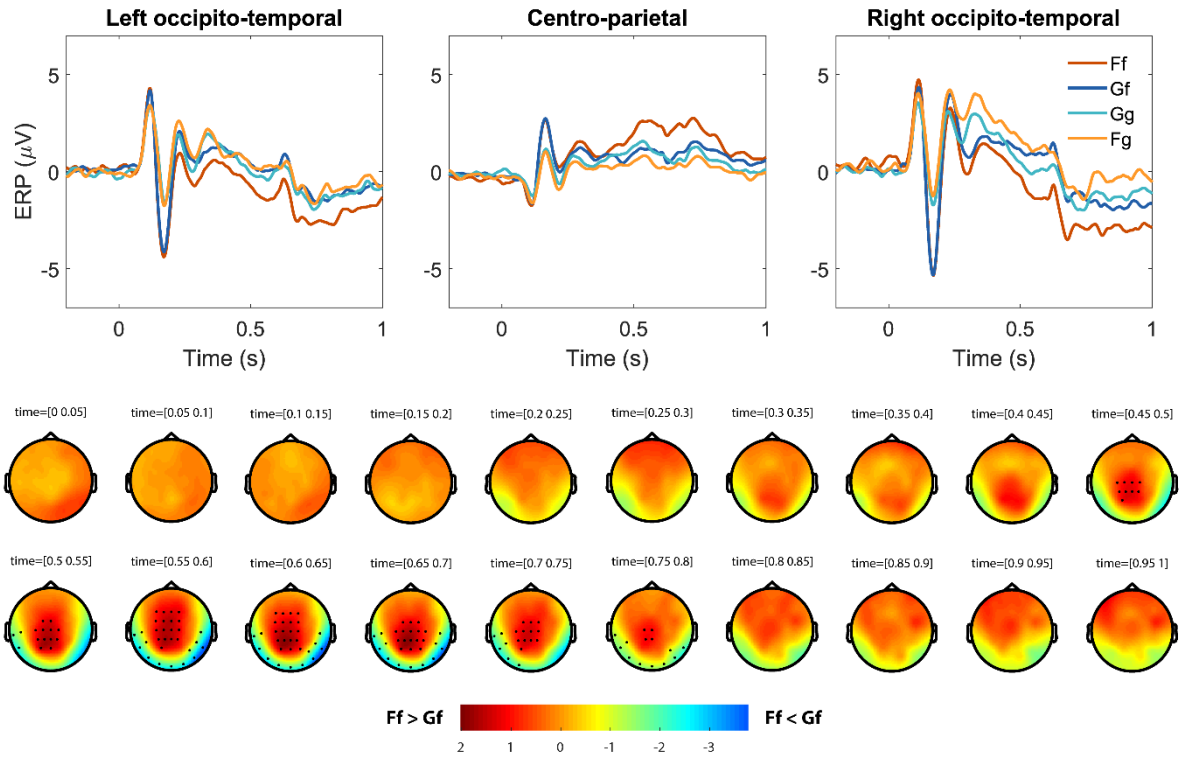

Figure 1.2. Grand average distractor-related EEG (ERP) at left and right occipito-temporal and centro-parietal regions are shown for the Ff, Gf, Gg and Fg conditions of Experiment 1 (top). Spatio-temporal properties of the Ff-Gf difference are provided at bottom, significant (P_{Clus} <0.05) effects are indicated by black dots.

We also performed a wavelet analysis of the alpha band activity in a time period between the retro-cue and distractor onset as well as after distractor onset. After retro-cue onset, we found increased bilateral alpha activity on the parieto-occipital electrodes in the FWMT trials as compared to GWMT trials. In the period after distractor onset there was a stronger alpha band desynchronization on the congruent as compared to incongruent trials both in the FWMT and GWMT, providing further support for enhanced processing of distractors in the congruent condition.

Experiment 2. The goal of the second experiment was twofold. First, to test whether the observed congruency effect on the P3b component was reflecting mnemonic processes associated with the distractor processing and separation of the distractor and WM content representations or alternatively, was associated with reactivation of the WM representations following distractor presentation in anticipation of the test stimulus. Second, test the robustness and reproducibility of the results obtained in the first experiment on a large group of participants (N=54). To this end, on

each trial in the delay period we inserted a second distractor stimulus that shared the object category of the first distractor and followed it with a 1000 ms delay. We reasoned that in case if distractor congruency effects on P3b component are indexing reactivation of WM representations in anticipation of the test stimulus we should see a reduced congruency-based modulation of P3b component after the first distractor, because of the presentation of a subsequent second distractor.

The results of the second EEG experiment were in close agreement with the findings obtained in the first experiment. Importantly, we found strong and sustained congruency effects on the EEG responses starting around 200 ms after the onset of both distractors and being most pronounced at the P3b component (Fig 1.3). In fact, congruency effects on the P3b component were more pronounced in case of the first distractor.

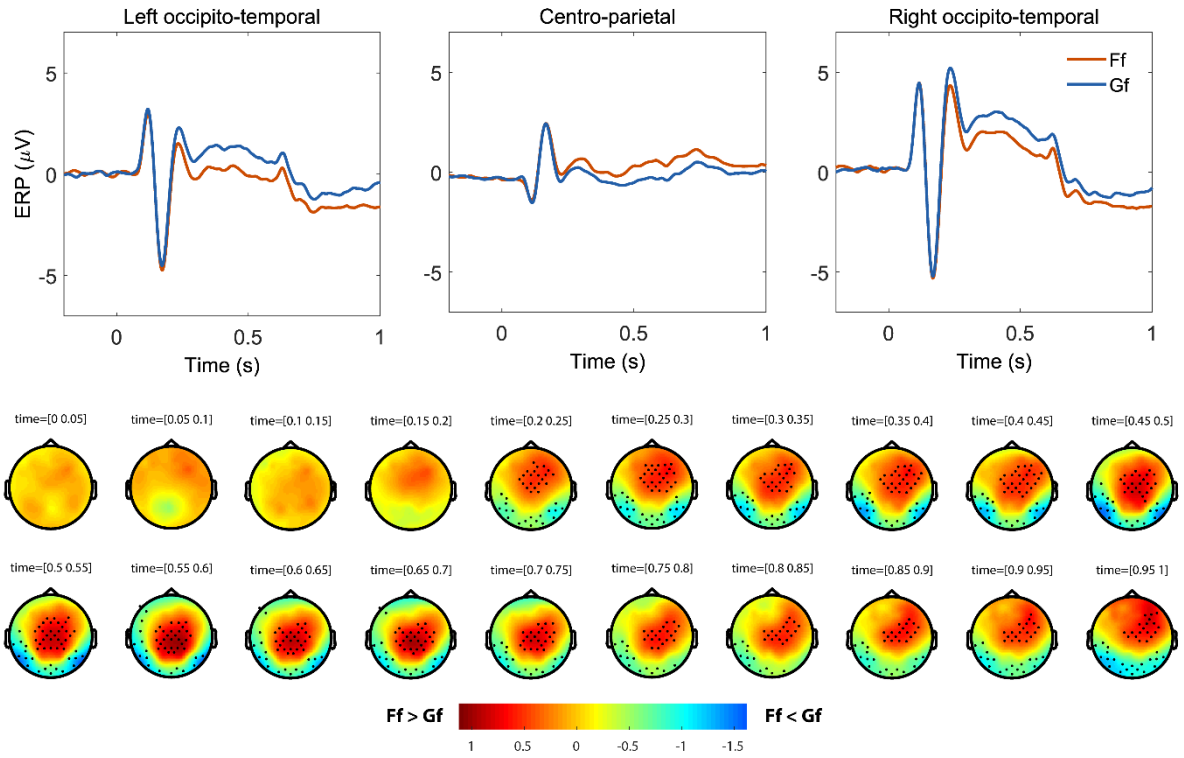

Figure 1.3. Grand average distractor-related EEG (ERP) at left and right occipito-temporal and centro-parietal regions are shown for the Ff and Gf conditions of Experiment 2 (top). Spatio-temporal properties of the Ff-Gf difference are provided at bottom, significant (P_{Clus} <0.05) effects are indicated by black dots.

In addition, we also found that similarly to the first EEG experiment, distractor-related alpha desynchronization was stronger in the congruent than in the incongruent trials for both distractors and being more pronounced after the first one (Fig. 1.4). Taken together, these results suggest that enhanced P3b and alpha desynchronization in case of congruent distractors might reflect increased demand on neural processes involved in separation and protection of WM representations from the interfering perceptual representations of the same-category distractors.

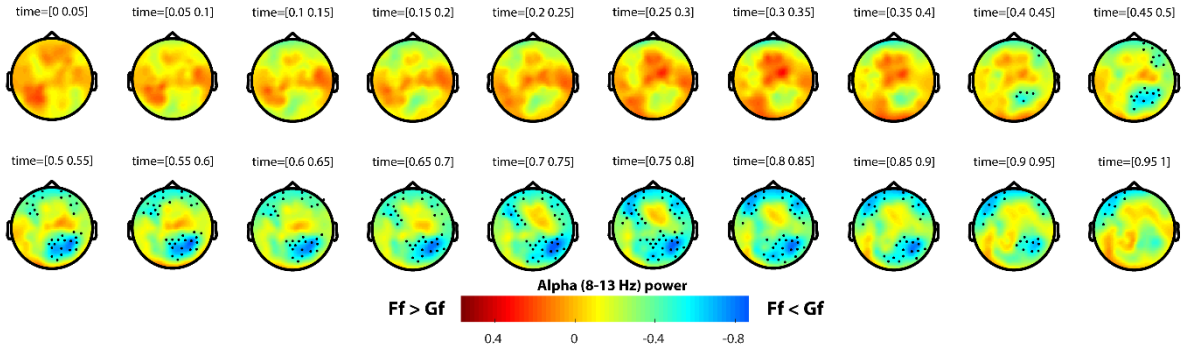

Figure 1.4. Difference of grand average distractor-related alpha-band (8-13 Hz) EEG activity between Ff and Gf conditions of Experiment 2. Significant (P_{Clus} <0.05) effects are indicated by black dots.

fMRI results

In agreement with previous findings, the fMRI results revealed dissociable networks of dorsal and ventral brain areas supporting WM for gratings (GWMT) and faces (FWMT), respectively (Fig. 1.5).

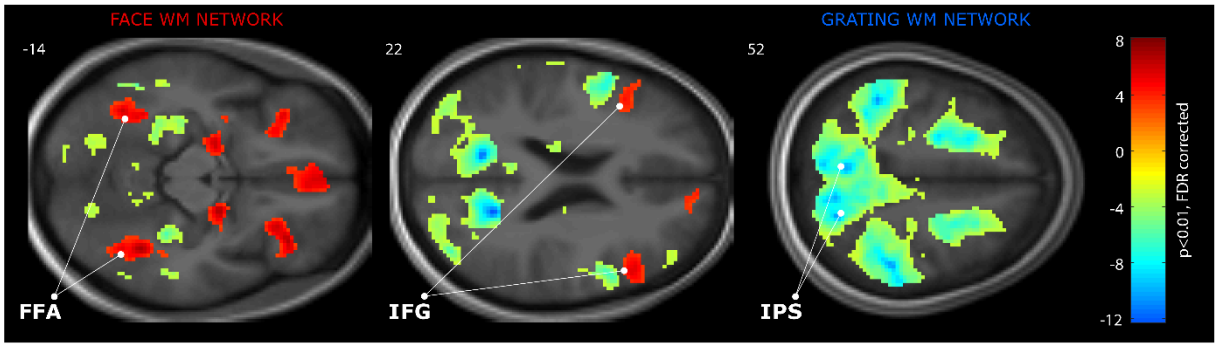

Figure 1.5. Face and grating WM network. Bilateral areas of the fusiform (z=-17 mm) and inferior frontal gyrus (z=22 mm) showed significantly higher fMRI responses measured during PROBE to FWMT than GWMT, while higher fMRI responses to GWMT than FWMT were found bilaterally in the intraparietal sulcus (z=52 mm). The colour bar represents *t* values (df=32). Statistical maps are displayed with p<0.05, two-tailed FDR whole-brain corrected at voxel level on axial slices of a mean structural image from all participants. MNI z-coordinates in mm are indicated in the upper left corner of each slice. FFA: fusiform face area; IFG: inferior frontal gyrus; IPS: intraparietal sulcus.

Neural responses in the core component of the grating WM network, the dorsal region of the Intraparietal Sulcus (IPS) were primarily determined by the WM content, i.e. there was a strong and sustained elevation of fMRI responses—extending into the delay period when distractors were presented—in case when gratings (GWMT) were actively maintained in WM as compared to faces (FWMT), both in the congruent (Gg) and incongruent (Gf) trials (Fig. 1.6). However, in the key structure of the face WM network, the Inferior Frontal Gyrus (IFG) sustained elevated fMRI responses in delay period were observed only on congruent trials, suggesting a dedicated role of IFG in interference resistance when both the memorized and distractor objects are faces (Ff).

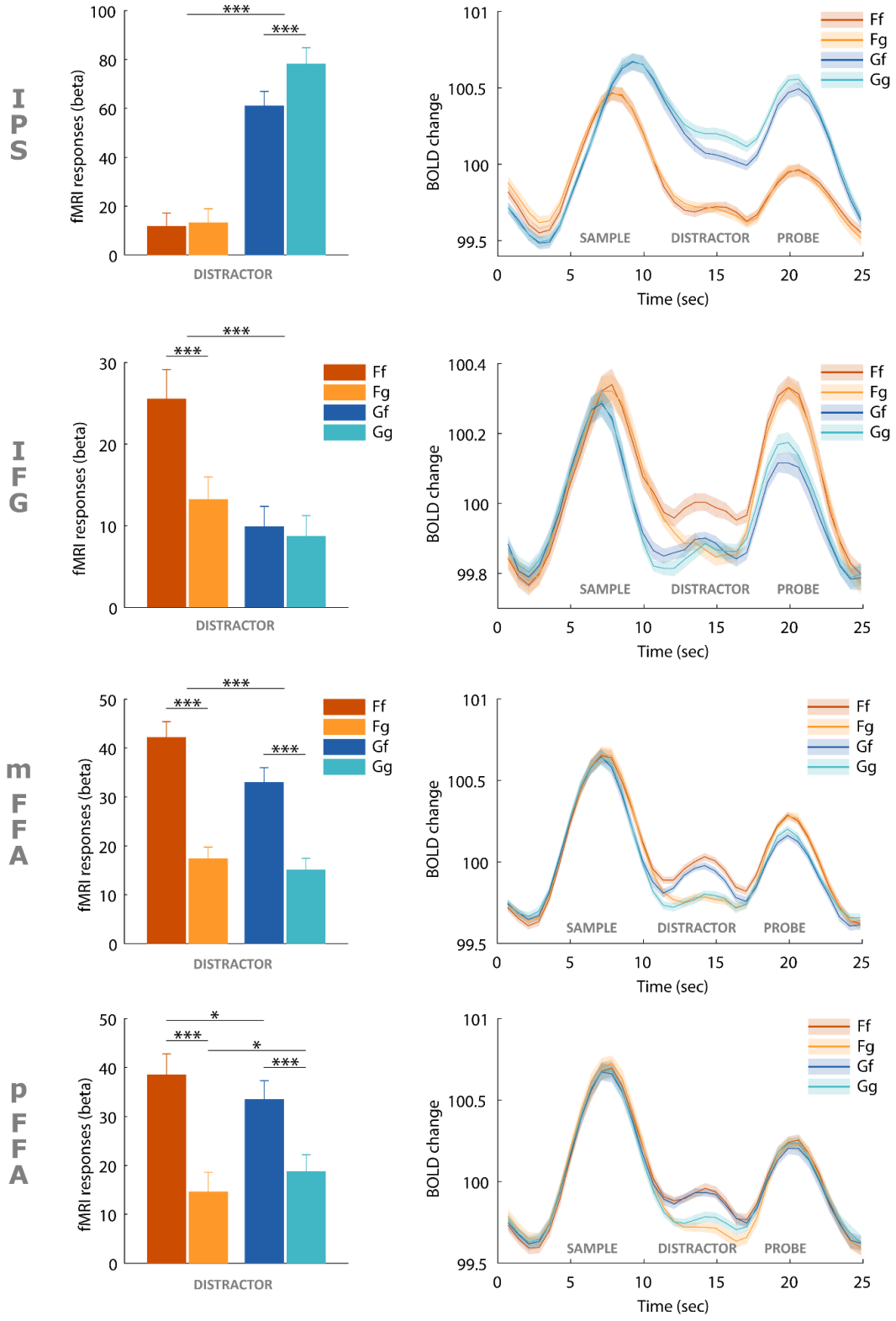

Figure 1.6. Grand average fMRI responses and BOLD time courses (±SE) in the core component of the face (IFG, mFFA, pFFA) and grating (IPL) WM network. Ff: FWMT with face (congruent) distractor; Fg: FWMT with grating (incongruent) distractor; Gf: GWMT with face (incongruent) distractor; Gg: GWMT with grating (congruent) distractor; IFG: inferior frontal gyrus; IPS: intraparietal sulcus; mFFA: middle fusiform face area; pFFA: posterior fusiform face area; *p < 0.05, ***p < 0.001.

Furthermore, fMRI responses in the core sensory areas of the face WM network, the middle and posterior Fusiform Face Area (FFA) were strongly modulated by the distractor category: face distractors (Ff and Gf) evoked larger fMRI responses than grating distractors (Fg and Gg) (see Fig. 1.6). Importantly, the results also revealed significant differences in WM-content-dependent modulation of the fMRI responses between the middle and posterior FFA. When faces (FWMT) as opposed to gratings (GWMT) had to be maintained in WM, fMRI responses to grating distractors (Fg) were reduced and unaltered in the posterior and middle FFA, respectively. Additionally, the results also revealed a significant positive correlation between the face identity WM performance in the congruent distractor condition (Ff) and the strength of the congruency effect on fMRI response modulations (Ff vs. Gf) in the IFG and in the middle FFA (Fig. 1.7). These results are consistent with the view that WM delay distractor resistance is achieved via feed-back processes that prioritize information processing in specific visual cortical areas containing the most precise task relevant WM representations in order to separate and protect them from the interfering distractor representations.

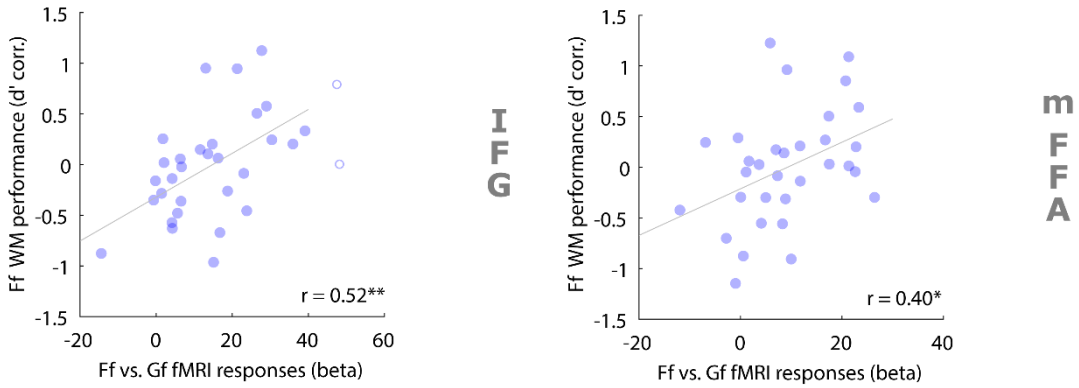

Figure 1.7. Relationship between face identity WM performance in the congruent distractor condition (Ff) and the strength of the congruency effect on fMRI response modulations (Ff vs. Gf) in the IFG and in the middle FFA. Circles represent individual participants; bivariate outliers are marked with open circles. Diagonal line indicates linear least-squares fit. Ff: FWMT with face (congruent) distractor; Gf: GWMT with face (incongruent) distractor; IFG: inferior frontal gyrus; mFFA: middle fusiform face area; *$p < 0.05$, **$p < 0.001$.

Conclusions

Taken together, our findings provided the first neuroimaging evidence that in the central visual field, where spatial attentional selection is inefficient, resistance to distractor interference during working memory maintenance might be achieved via feedback processes actively separating distractor representations from task-relevant mnemonic representations stored in the working memory. The object-separation-based distractor exclusion processes described in case of centrally presented distractors in our experiment are in sharp contrast to the sustained attentional selection processes found to be responsible for filtering out task irrelevant peripheral distractors and thus open a new direction towards understanding the neural basis of WM distractor resistance.

Publications:

Hermann, Petra ; Weiss, Béla ; Knakker, Balázs ; Madurka, Petra ; Vidnyánszky, Zoltán. NEURAL BASIS OF DISTRACTOR RESISTANCE DURING WORKING MEMORY MAINTENANCE. In: 16th Biannual Conference of the Hungarian Neuroscience Society. (2019) Paper: 83. Manuscript in preparation, to be submitted for publication by the end of February.

Knakker B, Kovács P, Maróti E, Vidnyánszky Z. VISUAL CORTICAL ALPHA OSCILLATIONS DURING OBJECT WORKING MEMORY – DISTRACTOR GATING OR ACTIVE MAINTENANCE. In: FENS Regional Meeting. (2017) P3-178

Balázs Knakker, Petra Kovács, Emese Maróti, Zoltán Vidnyánszky. Exploring EEG oscillations during opposing demands of working memory maintenance and distractor filtering. In: COFEES – Cortical Feedback Spring School. (2017) P29

Vidnyánszky, Z. Neural basis of visual noise and distractor filtering, COFEES: Spring School on cortical feed-back mechanisms in the central nervous system. Jena, Germany, 2017

Specific Aim 2

Neural basis of attentional selection and expertise in natural reading

Reading is a unique human ability that plays a pivotal role in the development and functioning of our modern society. In spite of this, our knowledge regarding the neural basis of reading remains limited. This is because natural reading is essentially an active sensory-motor process where visual sampling of the orthographic information is subserved by consecutive saccadic eye movements, yet, most previous research on reading impose strict gaze stability to control the time course of visual information processing and to avoid signal artefacts that eye movements generate. Although the passive presentation approach has revealed crucial properties of orthographic processing, it fails to capture the active nature of reading and thus might obscure some key aspects of neural processes subserving attentional selection and active sampling of visual information during natural reading.

Our goal was to develop a new methodological framework for single-trial analysis of fixation onset-related EEG activity (FREA) that enabled us to investigate visual information processing during natural reading. In particular, we aimed at using this new methodological approach to investigating key unresolved questions related to the neural basis of active sampling, attentional selection and reading expertise in normal and dyslexic readers.

2.1 Novel methods for investigation of brain mechanisms underlying natural reading

Background

Our knowledge about the neural background of natural reading is still very limited, because most previous neuroimaging studies have used fixed-gaze word-by-word paradigms. Eye movements are usually minimized during standard neuroimaging experiments to minimise artefacts originating from saccadic eye movements and to eliminate the potential effects of variable sampling of visual information. However, natural reading is a complex active process employing series of saccades and fixations for sampling of written text. Thus, there is a need for the investigation of neural mechanisms of reading under ecologically valid conditions. Recently, different research groups have

developed novel methods for research into natural reading by combining eye tracking (ET) and EEG. However, these methods did not account for the potential effects of eye-movement covariates, and all the approaches were based on sensor-space EEG data only, not allowing thus precise localization of brain sources underlying natural reading. To address these shortcomings, based on simultaneous recording of ET and EEG data and hierarchical linear modelling (HLM) of EEG, we developed a novel methodological framework for assessment of fixation-related brain activity while controlling for effects of covariates, and we also carried out a feasibility study on reliable localization of fixation-related brain activity by combining ET with EEG and magnetoencephalogram (MEG) recordings. We tested our HLM-based framework using a natural reading experiment during which an orthographic property of written text, i.e. interletter spacing was modulated, while the source localization approach was validated in another study in which the well-known N400 ERP component was tested under freewieving conditions.

Methods

In the first study, 24 undergraduate students (right-handed; 11 female; average age 22.33 years) read 32 Hungarian paragraphs at their own pace. Text was presented line by line using three different levels of letter spacing (LS): minimal spacing (MS ; 0.707 times the normal spacing); normal spacing (NS; the distance between consecutive characters is 1.16 times the width of the lowercase x); double spacing (DS; 2 times the NS). ET was performed at 1250 Hz, while EEG data were sampled at 500 Hz. ET data were processed by an adaptive algorithm. Behaviour of subjects was characterized by their reading speed (RS), saccade amplitude (SA), and fixation duration (FD). EEG recordings were cleaned using independent component analysis (ICA) by incorporating ET data. HLM of fixation-related EEG activity was performed in order to reveal the neural signatures of expertise-driven configural and visual processing load effects while controlling for eye-tracking variables that could also contribute to the variance of brain activity at single-trial level. At subject level, two different models were applied on single-trial FREA data. Effects of visual processing load (VPL) were tested by a multiple linear regression (MLR) model in which letter spacing was considered a continuous variable, while expertise-driven configural (EDC) effects were assessed with an analysis of covariance (ANCOVA) model using letter spacing as a categorical variable and by setting a -1 2 -1 contrast for the MS, NS and DS levels of letter spacing. Furthermore, we also analysed the correlation between effects of letter spacing on FREA and reading speed. To control for effects of eye-tracking covariates, 6 eye-tracking measures (current, first preceding and first following saccade amplitudes and fixation durations) were included in both MLR and ANCOVA models, taking into account the multicollinearity between these variables. Hence, this approach allowed for the assessment of pure letter spacing effects by regressing out the potential effects of saccade amplitude and fixation duration covariates. Group-level statistical analyses were performed using both threshold free cluster enhancement (TFCE) and spatio-temporal (2D) clustering to address the multiple comparisons problem.

In the second study, 18 young adults (right-handed; 11 female; average age 27.9 years) were instructed to read 248 four-word English sentences at their own pace and to make a judgement whether the last (target) word was plausible or implausible. All participants were native English, data were collected at MRC Cognition and Brain Science Unit, University of Cambridge, Cambridge, UK. ET, EOG, EEG and MEG (EMEG) data were recorded simultaneously. ET was performed at 250 Hz, while EEG (70 channels), MEG (204 planar gradiometers, 102 magnetometers) and EOG data were sampled at 1000 Hz. ET data were processed by an adaptive algorithm. Behaviour of subjects was

characterized by their reading speed (RS), saccade amplitude (SA), fixation duration (FD), total number of saccades (TNS) and percentage of regressive saccades (PRS). EMEG recordings were cleaned using independent component analysis (ICA) by incorporating EOG and ET data. Source localization of cleaned EMEG activity was carried out by using individual MRI anatomies, creating a 3-layer BEM forward solution and calculating the inverse solution using L2 minimum-norm estimates. Statistical differences between brain activity related to plausible and implausible target words were assessed in source space by spatio-temporal cluster-based permutation testing.

Results

In our first study, reading speed and fixation duration was reduced with the increase of letter spacing, suggesting that visual processing load is decreased as a result of increased inter-letter spacing. On the other hand, saccade amplitudes were increased with larger letter spacing. We found that orthographic processing is reflected in FREA in three consecutive time windows (120–175 ms, 230–265 ms, 345–380 ms after fixation onset) and the magnitude of FREA effects in the two later time intervals showed a close association with the participants' reading speed: FREA effects were larger in fast than in slow readers. Furthermore, these expertise-driven configural effects were clearly dissociable from the FREA signatures of visual perceptual processes engaged to handle the increased crowding (155–220 ms) as a result of decreasing letter spacing. Testing the potential effects of eye-movement covariates we found significant spatio-temporal effects of saccade amplitude and fixation duration on FREA. However, despite the observed linear correlations between letter spacing and saccade amplitudes, effects of letter spacing were found to be robust against such moderate level of multicollinearity.

In the study carried out for testing the localization of brain sources of natural reading, subjects read plausible sentences significantly faster (P=0.0009) compared to implausible sentences, and significantly larger TNS (P=0.0018), PRS (P=0.0033) and SA (P=0.0057) were found for implausible sentences. The latter trend was also observed for FD, but the difference did not reach the level of significance (P=0.2953). Visual inspection of fixation-related EMEG data revealed prominent deflections peaking around 90 and 250 ms in occipital and occipito-temporal sensors as well as a later component more extended in time (270-460 ms) in centro-parietal sensors. The latter component showed more negative-going deflection for the implausible words (N400). Cluster-based permutation testing resulted in a significant cluster (P_{Clus}=0.005) comprising medial temporal, inferior frontal and supplementary motor brain regions in the left hemisphere, with stronger activations for plausible compared to implausible words.

Conclusions

Our findings revealed significant effects of orthographic processing on FREA and that with increased reading skills orthographic processing becomes more sensitive to the configural properties of the written text. Based on thorough testing of eye-movement covariates and their effects on FREA, we also conclude that assessment of and correcting for potential effects of eye movements is essential for analysis of fixation-related brain activity.

To our knowledge, our approach applying the combination of ET and EMEG is the first attempt for localization of brain sources of natural reading. We could demonstrate that our approach produces clean EMEG data for source estimation, that the well-known N400 effect can be replicated, and that plausible spatio-temporal dynamics can be revealed during natural reading. Our results and

methodological framework may contribute to the deeper understanding of the neural mechanisms of natural reading, and may be useful for research on higher cognitive functions relying on active vision in general.

2.2 Natural reading in dyslexia

Background

Fluent reading comes as a result of extensive practice. Reading skills develop gradually from childhood to adolescence, and acquiring reading expertise has an overall effect on visual information processing and attentional selection. However, whether or how developmental dyslexia affects neural processes which underlie the evolvement of reading expertise remains unexplored. Here we addressed this question by investigating the hemispheric lateralization of fixation-related EEG components previously shown to be markers of reading expertise (see Special Aim 2.1, first study), that might correspond to the well-known word reading-related N1 ERP component exhibiting left hemispheric lateralization.

Methods

Twenty-four dyslexic (12 female; average age 24.79 years) and twenty-four control young adults (12 female; average age 23.04 years) participated in this experiment. Participants were instructed to read 250 isolated Hungarian sentences in a natural way at their own pace. Sentences were presented with five different letter spacing sizes, resulting in 50 sentences per condition. Spacing sizes were 0.7, 1, 1.3, 1.6 and 1.9 times the normal spacing and will be referred to as SP1, SP2, SP3, SP4 and SP5 respectively. Since spacing size was defined on sentence level, it remained the same even if a sentence was broken into two lines, presented separately. ET and EEG were recorded simultaneously during the experiment. ET was performed at 1250 Hz, while EEG data were sampled at 500 Hz. ET data were processed by an adaptive algorithm. Behaviour of subjects was characterized by their reading speed (RS), saccade amplitude (SA), and fixation duration (FD). EEG recordings were cleaned using independent component analysis (ICA) by incorporating ET data. Similarly to the first study in Specific Aim 2.1, HLM of fixation-related EEG activity (FREA) was performed in order to reveal the neural signatures of expertise-driven configural and visual processing load effects while controlling for eye-movement covariates. At subject-level, two different models were applied on single-trial FREA data. Effects of visual processing load (VPL) were tested by a multiple linear regression (MLR) model in which letter spacing was considered a continuous variable, while expertise-driven configural (EDC) effects were assessed with an analysis of covariance (ANCOVA) model using letter spacing as a categorical variable and by setting a -1 2 -1 -1 -1 contrast for the SP1, SP2, SP3, SP4 and SP5 levels of letter spacing. To investigate the hemispheric lateralization of FREA, the LI lateralization index was calculated by subtracting the activity of every right hemispheric channel from the contralateral left one and dividing this difference with their summed activity. Channels located along the midline were excluded from lateralization analyses, statistical analyses were carried out in our region of interest using posterior channel pairs (PO8-PO7, PO4-PO3, P6-P5, O10-O9, PO10-PO9, O2-O1, P8-P7, P4-P3, P10-P9). LI was assessed using the HLM framework. The eye-movement covariates were regressed out from LI at subject level. This was performed separately for the assessed SP1, SP2 and SP5 spacing conditions. Extent of lateralization was tested for all spacing×group combinations using one-sample t tests. Between-group effects were assessed for all the three spacing conditions separately with two-sample t tests, while between-spacing differences were tested for SP2-SP1 and SP2-SP5 condition

pairs for both dyslexic and control group separately by applying paired-samples t tests. Interaction between letter spacing and group factors was assessed by carrying out two-sample t tests on subject-level condition differences. Group-level statistical analyses were performed using both threshold free cluster enhancement (TFCE) and spatio-temporal (2D) clustering to address the multiple comparisons problem. TFCE was used to reveal the most prominent effects, therefore effects were reported primarily based on significant TFCE t-values. Since 2D clustering results may provide a better representation for the spatio-temporal extent of effects, properties of significant clusters were also reported.

Results

Speed and eye movement properties of natural reading

Statistical evaluation of reading speed revealed significant interaction between group and spacing factors (F=4.17, df=4, P=0.0029). Moreover, significant main effect was obtained for both group (F=24.24, df=1, P=0.000011) and spacing (F=34.3, df=4, P<0.00001) factors. Post hoc tests found significantly higher reading speed for the control group in all spacing conditions (P<0.001). Comparing the reading speed between the normal and modulated letter spacing levels revealed significantly faster reading for normal spacing compared to all increased letter spacings in control subjects ($P_{SP2vsSP3}$=0.00122, $P_{SP2vsSP4}$<0.001, $P_{SP2vsSP5}$<0.001), while in dyslexic subjects faster reading was found for normal spacing only when compared to SP4 (P=0.011) and SP5 (P<0.001) spacing conditions.

For saccade amplitude significant interaction between group and spacing factors (F=16.86, df=4, P<0.00001) as well as significant main effect of both group (F=23.13, df=1, P=0.000017) and spacing (F=657.89, df=4, P<0.00001) factors was obtained. Post hoc analyses found significantly larger saccades for the control group in all spacing conditions (P_{SP1}<0.03, and P<0.001 for the other four spacing levels), and significantly longer saccades for larger letter spacings for all spacing level combinations in both groups (P<0.001).

Similarly to saccade amplitude, significant interaction of group and spacing factors (F=4.4, df=4, P<0.002) was obtained for the duration of fixations. Main effect of group (F=8.88, df=1, P=0.0046) and spacing (F=385.2, df=4, P<0.00001) factors was also significant. Post hoc analyses found significantly longer fixation duration for dyslexic subjects compared to the control group in the decreased (P_{SP1}=0.0039) and the normal (P_{SP2}=0.026) letter spacing conditions only, the difference between the two groups was only marginal for the least increase (×1.3) of letter spacing (P_{SP3}=0.084; P>0.1 for SP4 and SP5). Considering the effects of letter spacing on fixation duration, significantly shorter fixation was found for larger letter spacings for all combinations of letter spacing levels in both groups (SP3 vs. SP4: P_{DYS}=0.0022, P_{CNT}=0.016; P<0.001 for the rest of the comparisons), except for the comparison of the two largest letter spacings (SP4 vs. SP5: P_{DYS}=0.092, P_{CNT}=0.85).

Fixation-related EEG activity (FREA)

Expertise-driven configural (EDC) effects

In our previous study (see Specific Aim 2.1, first study), we revealed significant expertise-driven configural effects in three consecutive time windows (120-175 ms in bilateral occipito-temporal and parietal, 230-265 ms in right occipito-temporal and 345-380 ms in left occipito-temporal and parietal regions). Here, significant EDC effects with similar spatio-temporal properties were found for the

control group (see Fig. 2.2.1). Early significant (P_{TFCE}<0.05) negative bilateral occipito-temporal and positive parieto-occipital effects were revealed in the 120-150 ms time range. Using 2D clustering, similar significant (P_{Clust}=0.01) effects were obtained with slightly increased spatio-temporal extent. These negative occipito-temporal t-values indicate more negative FREA amplitude in the normal spacing condition compared to altered ones. Significant (P_{TFCE}<0.05) bilateral positive occipito-temporal effects were found in the 225-260 ms time range, indicating increased FREA amplitude in normal spacing compared to the altered conditions. The corresponding significant (P_{Clust}=0.007) cluster showed larger spatio-temporal extent, indicating additional negative parietal effects in the same time range and occipital effects from 180 to 250 ms. Finally, late significant (P_{TFCE}<0.05) negative effects were revealed on three left occipito-temporal channels (PO7, P7, P5) in the 380-390 ms time range, however, the corresponding cluster did not reach the level of significance (P_{Clust}=0.059).

In dyslexics rather similar significant (P_{TFCE}<0.05, P_{Clust}=0.001) EDC effects were obtained from 115 to 150 ms in bilateral occipito-temporal and parietal regions (see Fig. 2.2.1). In the second time region, where controls showed strong and spatio-temporally extended effects, significant (P_{TFCE}<0.05) effects were revealed in the 245-250 ms time range only on three left occipito-temporal channels (PO9, PO7, O1) without the support of a significant cluster (P_{Clust}=0.11). In a later stage of FREA, significant (P_{TFCE}<0.05) right and left occipito-temporal effects were found in 320-345 ms and 370-390 ms time regions, respectively. These findings indicate more negative FREA in the normal spacing condition compared to altered ones. Both of these effects correspond to the same significant (P_{Clust}=0.004) cluster. This cluster also incorporates parietal channels with effects of opposite sign in the 330-395 ms time range. Despite the observed differences in the spatio-temporal extent of group-level EDC effects, there were no significant differences found between dyslexics and controls.

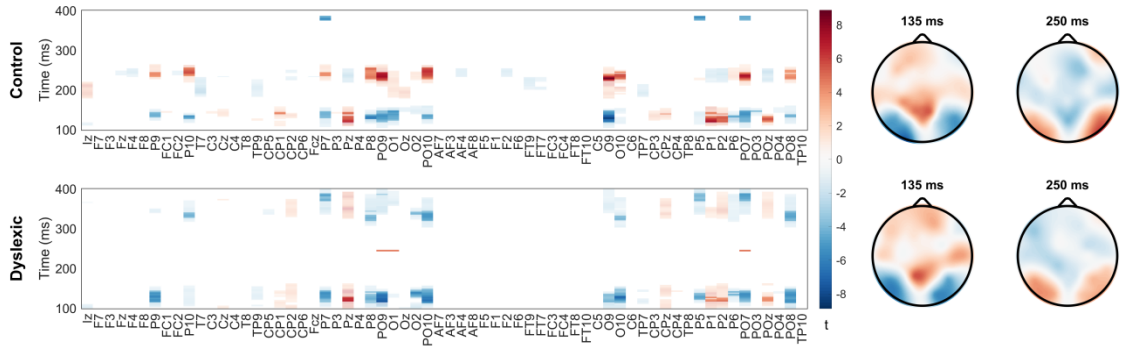

Figure 2.2.1. EDC effects revealed in control and dyslexic groups. The figure presents spatio-temporal maps of significant group-level t-values as well as topographic plots of t-values for time instances of special interest. Significant effects obtained using TFCE (P_{TFCE}<0.05) are presented as fully opaque, while significant 2D clusters (P_{Clust}<0.05) are shown with lowered opacity.

Visual processing load (VPL) effects

In our previous study, we revealed visual processing load (VPL) effects in right occipito-temporal and parietal regions in the 155-220 ms time window. Based on these findings, here were investigated VPL effects in the 170-210 ms time range. Significant positive bilateral occipito-temporal and negative centro-parietal effects were revealed from 170 to 210 ms in both control (P_{TFCE}<0.05, P_{Clust}=0.001) and dyslexic (P_{TFCE}<0.05, P_{Clust}=0.00001) groups (Fig. 2.2.2). The revealed occipito-temporal effects indicate that the amplitude of negative FREA deflection decreases as spacing size increases. Negative

centro-parietal effects however indicate that by increasing the spacing size, the positive FREA deflection decreases. There were no significant between-group differences found.

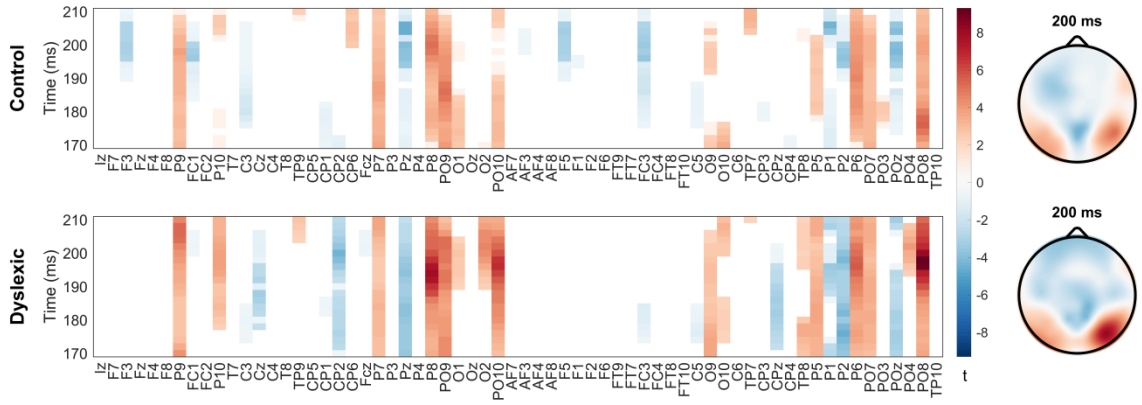

Figure 2.2.2. VPL effects in control and dyslexic groups investigated from 170 to 210 ms after fixation onset. The figure presents spatio-temporal maps of significant group-level t values as well as topographic plots of t-values for time instances of special interest. Significant effects obtained using TFCE (P_{TFCE}<0.05) are shown as fully opaque, while significant 2D clusters (P_{Clust}<0.05) are provided with lowered opacity.

FREA of occipito-temporal clusters indicated linear trend of normal and increased spacing sizes in several time windows, however, FREA in the SP1 condition did not follow this trend generally, indicating that there may be a linear effect of letter spacing exclusive to increased spacings. To this end, VPL effects were tested with the omission of the decreased spacing (SP1) condition (see Fig. 2.2.3). Significant (P_{TFCE}<0.05) bilateral positive occipital and occipito-temporal, as well as, negative centro-parietal effects were revealed from 115 to 170 ms for the control group. Results indicate a decrease in the amplitude of negative occipital and occipito-temporal and positive centro-parietal activity with increasing spacing size. The corresponding significant cluster (P_{Clust}<0.00001) further extends to the 170-210 time range on right occipito-temporal channels, which is in accordance with the above reported findings of the VPL analysis with all spacing conditions. Furthermore, significant (P_{TFCE}<0.05) negative occipital and occipito-temporal, as well as positive parietal effects were revealed in the 220-275 ms time range with the corresponding significant (P_{Clust}=0.001) cluster slightly extended in time. These findings reflect a decrease in positive occipital, occipito-temporal and negative centro-parietal FREA amplitude as spacing size increases. Finally, significant (P_{TFCE}<0.05) positive left occipito-temporal and left parietal effects were found in the 385-400 ms time window. The related significant (P_{Clust}=0.035) cluster covers the same effects, but it has a larger extent both in time (340-400 ms) and space, it includes additional weak negative occipito-parietal effects. These results indicate an increase in absolute amplitude of left occipito-temporal and occipito-parietal FREA as spacing size increases.

In dyslexics, similarly to the control group, significant (P_{TFCE}<0.05, P_{Clust}=0.035) VPL effects were revealed from 100 to 195 ms in bilateral occipital, occipito-temporal and centro-parietal regions, representing decrease of absolute FREA amplitude as spacing size increases. Furthermore, in the second time window, significant (P_{TFCE}<0.05) negative effects were revealed at 245 ms on three channels (O2, PO10, O10). The corresponding significant (P_{Clust}=0.025) cluster was much more extended in both space and time, incorporating occipital and occipito-temporal channels from 225 to 285 ms. These findings show a decrease in positive occipital and occipito-temporal FREA amplitude

as spacing size increases. Finally, significant (P_{TFCE}<0.05) positive occipital, occipito-temporal and parietal effects were revealed in the 320-400 ms time range, with the corresponding significant (P_{Clust}=0.001) cluster extending to the 295-400 ms time range and incorporating negative t-values in the centro-parietal region. These results indicate an increase in the positive occipito-temporal and negative occipito-parietal FREA amplitudes, as well as, a decrease in negative parietal FREA amplitude as spacing size increases. Despite visible disparity between dyslexic and control groups, there were no statistically significant differences revealed.

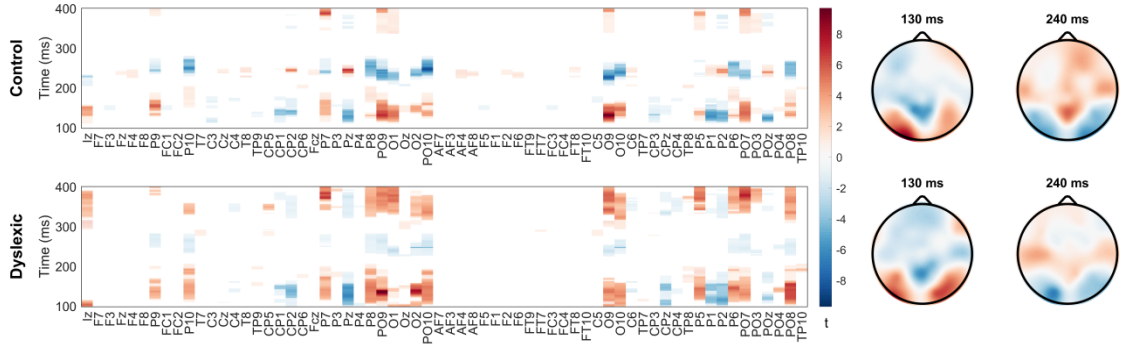

Figure 2.2.3. VPL effects in control and dyslexic groups using only the normal and increased spacing conditions. The figure presents spatio-temporal maps of significant group-level t-values as well as topographic plots of t-values for time instances of special interest. Significant (P_{TFCE}<0.05) effects obtained using TFCE are presented as fully opaque, while significant (P_{Clust}<0.05) 2D clusters are shown with lowered opacity.

Lateralization of FREA

Fig. 2.2.4 presents the grand average lateralization index (LI) for each spacing condition of both groups, computed using three occipito-temporal channel pairs (PO10-PO9, PO8-PO7, P8-P7). The time window of interest was defined based on zero-crossings of LI (control group, normal spacing condition). The time of the first LI zero-crossing (72 ms) preceding the first negative FREA peak around 140 ms and the time of the first LI zero-crossing (278 ms) following the second positive FREA peak around 245 ms were used to define the time boundaries of statistical evaluation.

Statistical results for FREA lateralization in the normal spacing condition are shown on Fig. 2.2.5. Analyses were carried out in the time range between the zero-crossing times of control normal spacing LI (72-278 ms). In controls significant (P_{TFCE}<0.05, P_{Clust}=0.002) leftward lateralization of negative FREA was revealed from 85 to 140 ms on all investigated posterior channel pairs with similar spatio-temporal characteristics in both statistical analyses. Furthermore, significant (P_{TFCE}<0.05, P_{Clust}=0.00001) rightward lateralization of negative FREA was found from 160 to 205 ms in posterior regions, spatio-temporal extent of the corresponding significant cluster was in accordance with TFCE results. Finally, significant (P_{TFCE}<0.05) rightward lateralization of positive FREA was revealed at 245 ms on three occipito-temporal channels with the corresponding significant (P_{Clust}=0.041) cluster found in the 240-260 ms time window including additional channels even in occipital and parietal regions.

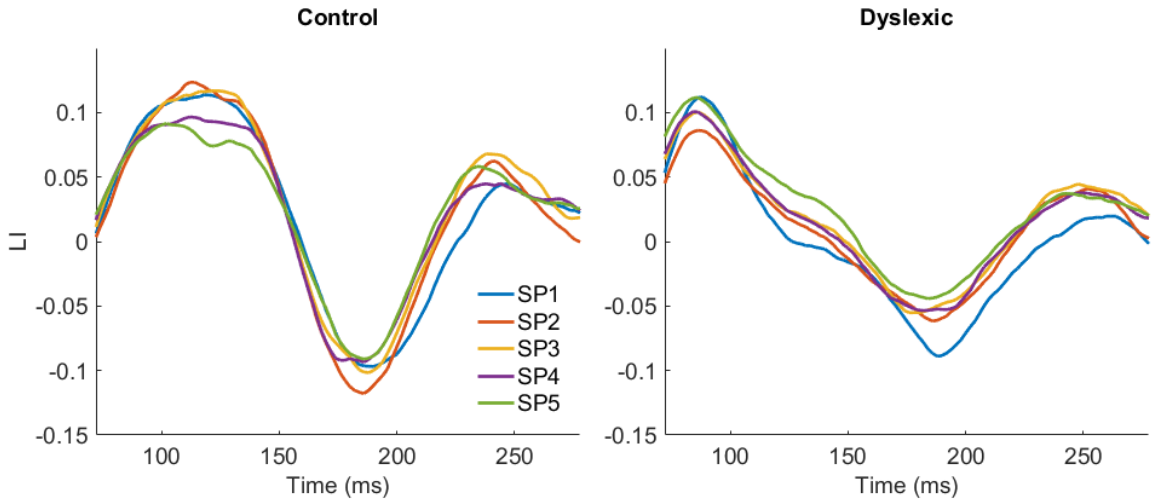

Figure 2.2.4. Grand average lateralization index (LI) is shown for each spacing condition (SP1, SP2, SP3, SP4, SP5) and for both groups between the nearest zero-crossing times (72-278 ms) around the first negative and second positive FREA peaks of the control group in the normal spacing condition (SP2). LI was calculated using three occipito-temporal channel pairs (PO10-PO9, PO8-PO7, P8-P7).

In dyslexics significant (P_{TFCE}<0.05) rightward lateralization of negative FREA was found from 180 to 200 ms on occipital, occipito-temporal and parietal channel pairs. The corresponding significant (P_{Clust}=0.007) cluster was revealed from 170 to 205 ms, including additional channels in the occipito-temporal region. To compensate the aforementioned drawbacks of cluster statistics, group effects were further investigated in dyslexics by performing statistical tests in limited time windows based on control results. Investigation of early effects in the time range of the significant control-group cluster (80-140 ms) did not reveal significant effects in dyslexics (P_{Clust}=0.17). When testing late effects, the time range of the significant control-group cluster was extended with 10 ms (240-270 ms) to control for the between-group latency difference of the corresponding FREA peaks. Limiting the statistical testing to this time window, significant (P_{TFCE}<0.05, P_{Clust}=0.024) rightward lateralization of FREA was revealed in dyslexics from 260 ms to 265 ms in occipito-temporal channels with 2D clustering results being more extended in time.

Between-group differences of LI were tested in the time range of significant clusters found in controls, revealing significantly (P_{Clust}=0.037) weaker leftward lateralization of FREA in dyslexics compared to controls from 95 to 125 ms in occipital, occipito-temporal and parietal regions with 2D clustering. Using TFCE, significant (P_{TFCE}<0.05) results were obtained with reduced spatio-temporal extent from 100 to 110 ms on occipito-temporal and parietal channel pairs. There were no significant differences revealed between the two groups when tested in the time range of the second (P_{Clust}=0.095) and third (no cluster formed) clusters that reached significance in controls.

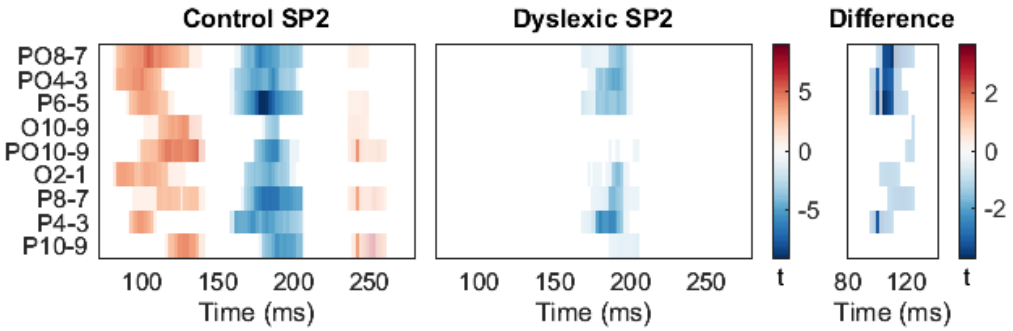

Figure 2.2.5. Lateralization of FREA on posterior channel pairs in the normal spacing (SP2) condition. The figures present spatio-temporal maps of significant group-level t-values. Significant (P_{TFCE}<0.05) effects obtained using TFCE are presented as fully opaque, while significant (P_{Clust}<0.05) 2D clusters are shown with lowered opacity.

The effects of letter spacing on FREA lateralization were tested by comparing LI between the SP2 and SP5 as well as between SP2 and SP1 conditions. Considering the difference of LI between the normal (SP2) and largest (SP5) spacing conditions (Fig. 2.2.6) significantly (P_{TFCE}<0.05) larger lateralization of FREA was revealed in SP2 compared to SP5 at 115 ms and from 120 to 125 ms in occipital and occipito-temporal regions only in controls, using TFCE in the time range between the closest zero-crossings of normal spacing LI (72-156 ms). Both time ranges of significant t values are corresponding to a common significant (P_{Clust}=0.023) cluster found in the 105-140 ms time window further extending to parietal channels. Furthermore, significant (P_{TFCE}<0.05, P_{Clust}=0.02) interaction was revealed between the SP2-SP5 conditions and the two groups from 120 to 145 ms on occipital and occipito-temporal channel pairs, with 2D clustering results slightly extended in time. This indicates larger SP2-SP5 difference of FREA lateralization in controls compared to dyslexics.

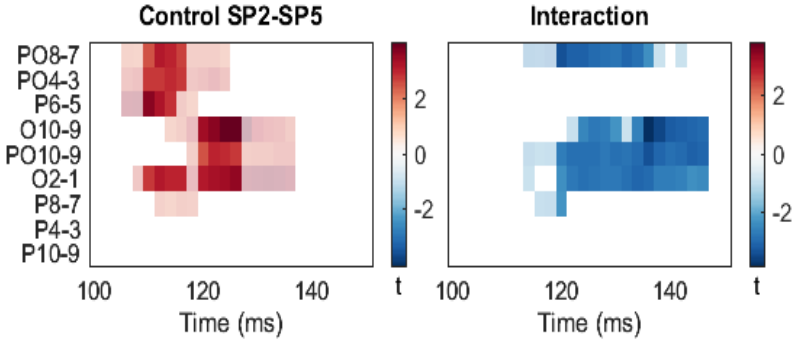

Figure 2.2.6. Comparing normal spacing (SP2) lateralization index (LI) with the largest (SP5) spacing LIs. The figures present spatio-temporal maps of significant group-level t-values. Significant (P_{TFCE}<0.05) effects obtained using TFCE are presented as fully opaque, while significant (P_{Clust}<0.05) 2D clusters are shown with lowered opacity.

Since grand average FREA lateralization (see Fig. 2.2.4) showed differences between the normal (SP2) and decreased (SP1) spacing conditions, these were also subjected to statistical analyses. Investigating lateralization measures between normal spacing zero-crossing times corresponding to late normal spacing effects revealed in controls, significantly (P_{TFCE} < 0.05) stronger lateralization of positive FREA was revealed in SP2 compared to SP1 from 240 to 245 ms on occipito-temporal channel pairs (PO10-PO9, P8-P7, P10-P9) in controls, with the corresponding significant (P_{Clust}=0.032)

cluster obtained in the 235-245 ms time range. Testing the SP2-SP1 difference in dyslexics using the same time window, significantly (P_{TFCE}<0.05) stronger lateralization of positive FREA was revealed in SP2 compared to SP1 from 255 to 260 ms on occipital and occipito-temporal channel pairs (PO8-PO7, O10-O9, PO10-PO9) only with TFCE. Furthermore, testing the SP2-SP1 difference in dyslexics within the time window where the significant cluster was found in controls revealed significantly (P_{TFCE}<0.05, P_{Clust}=0.035) stronger lateralization of positive FREA in SP2 compared to SP1 from 235 to 245 ms in occipito-temporal regions, slightly reduced in time when using 2D clustering. Finally, lateralization of negative FREA was revealed to be significantly (P_{TFCE}<0.05) smaller in SP2 compared to SP1 from 190 to 205 ms on occipito-temporal and parietal channel pairs in the dyslexic group, with the corresponding significant (P_{Clust}=0.035) cluster being spatio-temporally more extended.

Conclusions

Our results reveal that in dyslexics the early N1 component of the fixation-related EEG activity is evenly distributed over the two hemispheres as opposed to its strong left-hemispheric lateralization observed in the control readers. These findings provide the first experimental evidence for disturbed reading expertise-related hemispheric specialization of orthographic processing in dyslexia and thus will represent a major advance in the understanding of the neural background of reading impairments.

2.3 Lateralization of alpha-band EEG activity during natural reading

Background

Lateralization of alpha oscillations is closely related to visuospatial attention deployment and inhibition of distractor stimuli, therefore, their examination is crucial to understand the neural processes underlying natural reading.

Methods

We investigated the effects of letter spacing on lateralization of baseline and evoked alpha-band (8-13 Hz) power by analysing fixation-related brain activity recorded during the saccadic reading experiment carried out for Specific Aim 2.1, first study.

Results

We found rightward lateralization of occipito-temporal baseline alpha power that was significantly weaker in the increased spacing condition. Furthermore, we obtained significantly stronger lateralization of evoked alpha synchronization and desynchronization in normal spacing condition compared to altered spacings from 100 to 180 ms and from 220 to 290 ms after fixation onset, respectively.

Conclusions

Our findings may indicate that experienced readers perform better at visuospatial attention deployment when reading text with familiar orthographic properties.

Publications:

Weiss, B ; Knakker, B ; Vidnyanszky, Z. Visual processing during natural reading. SCIENTIFIC REPORTS 6. (2016) Paper: 26902

Nárai, Ádám ; Vidnyánszky, Zoltán ; Weiss, Béla, Eye-movement correlates of fixation-related EEG activity in natural reading. In: 41st European Conference on Visual Perception. (2018) Paper: 114M

Weiss, Béla ; Dreyer, Felix ; van Casteren, Maarten ; Hauk, Olaf. Investigating brain mechanisms underlying natural reading by combining eye tracking, EEG and MEG. In: Annual, Meeting of the Organization for Human Brain Mapping - Annual Meeting of the Organization for Human Brain Mapping POSTER LISTINGS. (2017) Paper: 1769

Farkas, David ; Vidnyánszky, Zoltán ; Weiss, Béla. The effects of interletter spacing on eye movements during natural reading in dyslexic and control adults. In: 41st European Conference on Visual Perception. (2018) Paper: 112M

Weiss, Béla ; Nárai, Ádám ; Vidnyánszky, Zoltán. READING EXPERTISE-RELATED HEMISPHERIC SPECIALIZATION OFORTHOGRAPHIC PROCESSING IS IMPAIRED IN DEVELOPMENTAL DYSLEXIA. In: 16th Biannual Conference of the Hungarian Neuroscience Society. (2019) Paper: 75. Manuscript in preparation, to be submitted for publication by the end of February.

Weiss, Béla ; Nárai, Ádám ; Vidnyánszky, Zoltán. Letter spacing modulates lateralization of EEG alpha oscillations during natural reading. In: 41st European Conference on Visual Perception. (2018) Paper: 97M

Specific Aim 3

3.1. Interocular suppression in amblyopia

In this specific aim, we set out to study the brain processes contributing to interocular suppression in amblyopia using EEG. In the first set of EEG experiment performed on the amblyopic patients, participants had to monitor small visual transients appearing randomly either binocularly (BO) or selectively for one eye (AE or FE), while a rich visual stimulus (a face) was continuously presented for both eyes, to stabilize binocular vision. Our results revealed a late (between 300-500 ms after the onset of the visual transient) ocular differences in ERP responses (Fig. 3.1.1) and alpha oscillations that might be considered as EEG markers of amblyopic interocular suppression.

To provide further support for our interpretation of the observed ocular differences in ERP responses and alpha oscillations as markers of amblyopic interocular suppression, we decided to pursue a computer-based dichoptic visuomotor coordination training of the amblyopic patients involved in the first experiment and after its completion repeated the EEG measurements. We reasoned that in case the late component of ocular differences in ERP responses and alpha oscillations observed before training can indeed be considered as markers of interocular suppression one would expect an attenuation of these amblyopic effects as a result of training-induced improvements in amblyopic vision.

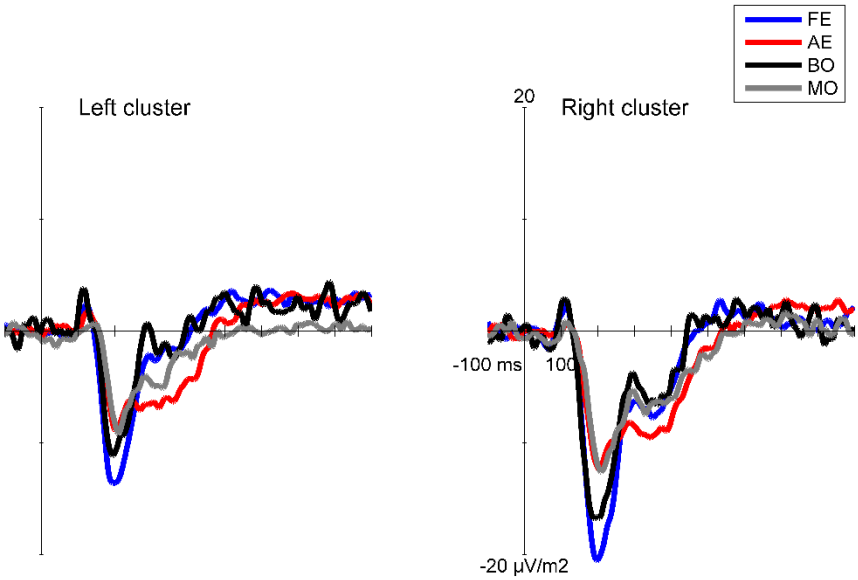

Figure 3.1.1. Grand average EEG activity for amblyopic (AE) and fellow eyes (FE) as well as for the binocular (BO) condition.

The training procedure and post-training ERP measurements in 17 amblyopic patients have been completed. Results revealed significant improvement in visual acuity of the amblyopic eye in the cases of both distance (approx 0,5 line on the acuity chart) and near acuity (approx 1.5 lines of the acuity chart). Stereoacuity has also improved significantly with an average change of 3.4 log arcseconds. Full analysis of the electrophysiological data is expected to be finished by the end of March 2019. We have to admit that research progress within this project has been slower than expected. This is because dr. Éva Bankó, who is a key member of the team working on the amblyopia projects has been on maternity leave and was able to work on the project only part time. Nevertheless, we are confident that the research goals we undertook within this specific aim could be achieved by the end of June 2019. All the required resources are available at the research group for the successful completion of this very important project.

3.2. Amblyopic deficits in natural sampling of visual information

Background

Amblyopia is the most common cause of vision impairment in a single eye among children and young adults. However, how amblyopia affects brain activity in natural viewing conditions still remains to be explored. To address this shortcoming, here we assessed how amblyopia modulates the early fixation-related EEG response during active scanning of human faces.

Methods

Twenty young amblyopic adults (5 female; 22-55 years; 10 anisometropic, 7 strabismic) participated in this study. Participants were instructed to scan probe stimuli containing 5 human faces (freeviewing task), and to decide whether the test face was presented on the preceding probe (fixed-eyes task). Subjects' eye movements and EEG were recorded simultaneously. To obtain test face-related EEG (TEEG) and fixation-related EEG activity (FREA), epochs were triggered to the onset of test faces and to saccade endings, respectively. EEG data was analysed using hierarchical linear

modelling to regress out the potential effects of covariates (fixation duration, fixation position, saccade amplitude, saccade angle, reaction time). Effects of amblyopia on FREA were evaluated separately for within- and between-face saccades, and correlation analyses between FREA/TEEG features and visual acuity was also carried out.

Results

Although the duration of fixations did not differ significantly between the amblyopic and fellow eyes, and only a marginal difference was found in the case of saccade amplitude (Fig. 3.2.1), EEG data was analysed using hierarchical linear modelling (HLM) to regress out the potential effects of eye movement covariates. Grand average FREA and TEEG are presented on Fig. 3.2.2. For within-face saccades significantly weaker fixation-related EEG response was found for the amblyopic eye from 35 to 105 ms in occipital and from 65 to 110 ms in occipito-temporal channels (Fig. 3.2.3). Considering between-face saccades, the same trend was observed, but from 25 ms to 95 ms in occipital and from 65 ms to 105 ms in occipito-temporal electrodes (Fig. 3.2.3). Moreover, in the case of within-face saccades, the significant effect of amblyopia on fixation-related EEG in right occipito-temporal channels significantly correlated with the visual acuity difference between the two eyes (Fig. 3.2.4a).

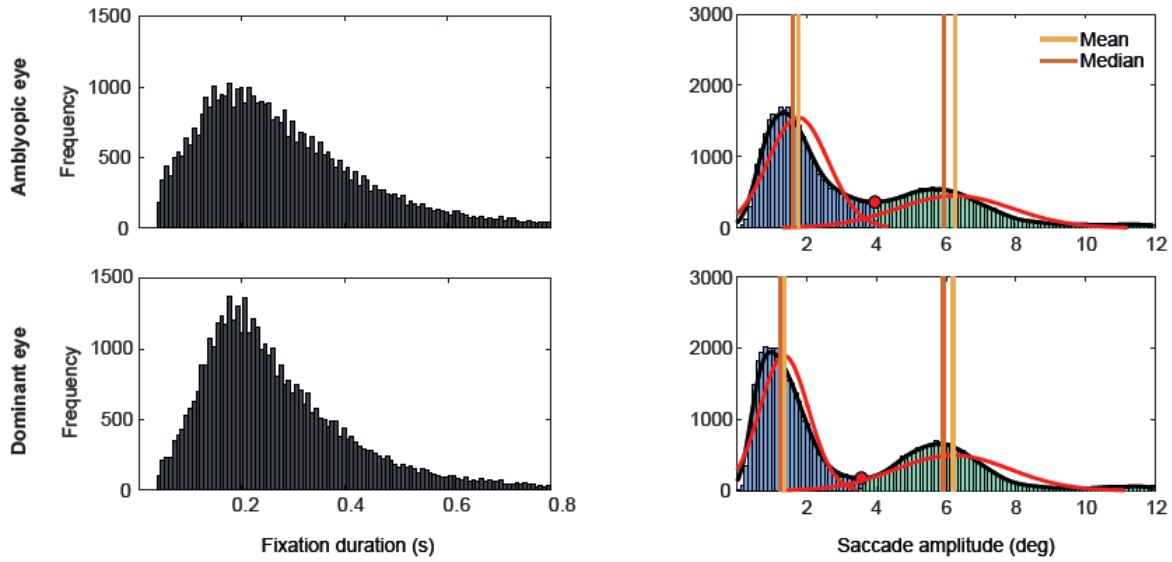

Figure 3.2.1. Fixation duration and saccade amplitude histograms for amblyopic and dominant eyes. The duration of fixations did not differ between the two eyes. The amplitude of saccades did not differ in the case of between-face saccades (green part of the histogram), while larger saccades were found for the amblyopic eye when considering within-face saccades (p_{Bonf}=0.04, blue).

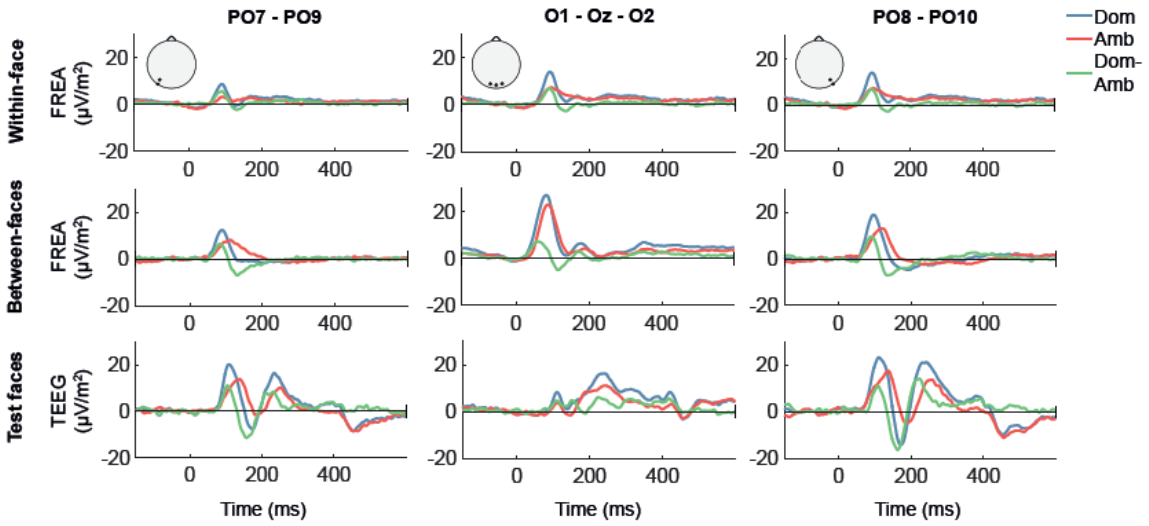

Figure 3.2.2. Grand average fixation-related EEG activity (FREA) for within- and between-face saccades and grand average EEG activity triggered to the onset of test faces (TEEG). Dom: dominant eye; Amb: amblyopic eye; Dom-Amb: dominant-amblyopic eye.

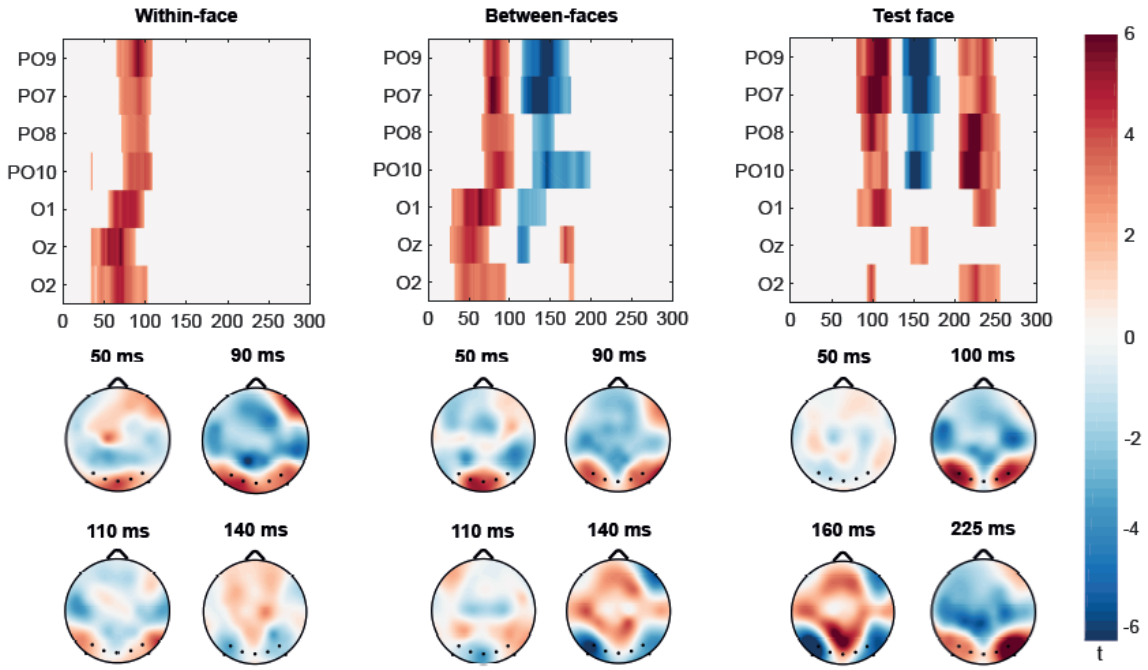

Figure 3.2.3. Group-level statistical results of HLM showing spatio-temporal distribution of t values for occipital and occipito-temporal channels as well as full topography of t values at time points of special interest. Significant dominant-amblyopic effects: within-face p_{C1}=0.01; between-face p_{C1}=0.007, p_{C2}=0.006; test face: p_{C1}=0.015, p_{C2}=0.017, p_{C3}=0.007.

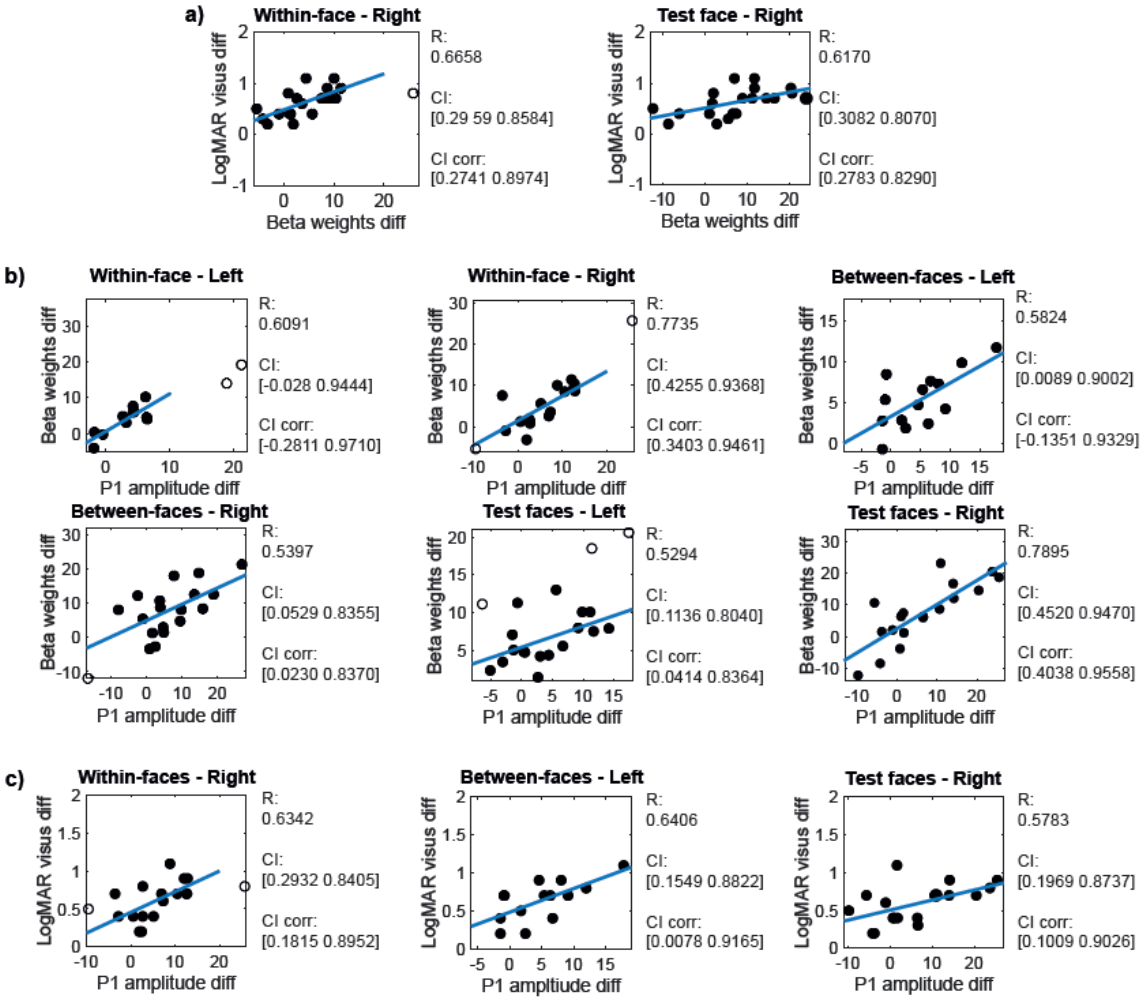

Figure 3.2.4. Scattergrams between visus and HLM beta weight differences (a), between HLM beta weight and P1 amplitude differences (b), and between visus and P1 amplitude differences. Difference of visus was obtained as amblyopic-dominant, while dominant-amblyopic was used for EEG measures. Right: right occipito-temporal; Left: left occipito-temporal; R: Spearman's correlation coefficient, CI: confidence interval; CI corr: CI with multiple comparisons correction.

Conclusions

The present experiment provided the first experimental results on visual information processing during natural viewing in amblyopia. Even though eye movement recordings revealed only marginal differences between the fixation patterns of the amblyopic and fellow eyes, there was marked reduction in early fixation-related EEG activity measured during sampling of visual information by the amblyopic eye as compared to the fellow eye.

Publications:

Gerendás, Péter ; Bankó, Éva M. ; Vidnyánszky, Zoltán ; Weiss, Béla. EARLY FIXATION-RELATED EEG ACTIVITY IS REDUCED IN AMBLYOPIA DURING FREEVIEWING OF HUMAN FACES. In: 16th Biannual Conference of the Hungarian Neuroscience Society (2019) Paper: 84. Manuscript in preparation, to be submitted for publication by the end of February.